

## TITANIUM SILICIDE FORMATION IN PRESENCE OF OXYGEN

C. NOBILI, F. NAVA, G. OTTAVIANI, M. COSTATO

*Dipartimento di Fisica Universita' di Modena, via Campi 213/a, I-41100 Modena, Italy*

G. DE SANTI AND G. QUEIROLO

*SGS, via Olivetti 2, I-20041 Agrate Brianza, Milano, Italy*

*(Received December 24, 1990; in final form November 18, 1991)*

In-situ resistivity vs. temperature, Rutherford backscattering spectrometry, Auger electron spectroscopy and X-ray diffraction measurements have been performed in order to study the effects arising from the presence of oxygen in the annealing ambient on the integrity of amorphous films of  $TiSi_x$ , with  $x$  ranging from 1.45 to 2.1. Crystallisation occurs around 400 C. The presence of oxygen produces the formation of silicon and titanium oxide around 500 C. Critical analysis of the experimental results have indicated that metal oxidation is inhibited when an excess of silicon is present, which suggests the use of a sputtered Si coating cap as a medium capable of effectively decoupling the silicide film from oxygen. This avoids unwanted Ti oxidation even in heavily oxygen contaminated ambients up to the highest temperatures used for the formation of low resistivity titanium disilicide.

*Key Words: Titanium Silicide, rf Sputtering, Resistivity vs. Temperature, Rutherford Backscattering Spectrometry, Auger Spectroscopy, X-Ray Diffraction*

### INTRODUCTION

Among the refractory metal/silicon compounds, titanium-disilicide is the material with the lowest electrical resistivity at room temperature<sup>1,2</sup>. As a consequence it is preferred when interconnections in silicon integrated electronic devices are required. The silicon-titanium phase diagram includes five stable compounds<sup>2,11</sup>:  $TiSi_2$ ,  $TiSi$ ,  $Ti_5Si_4$ ,  $Ti_5Si_3$ ,  $Ti_3Si$ , and the disilicide is the one of interest. It has two different crystalline structures: one orthorhombic base-centered C49 (bc C49  $TiSi_2$ ) structure<sup>3</sup>, which is formed after low temperatures anneals (around 500 C), and the other orthorhombic face-centered C54 (fc C54  $TiSi_2$ ) structure<sup>4</sup>, which is formed above 700 C. The fc C54  $TiSi_2$  structure has the lowest resistivity of the two.

Several techniques have been employed for the formation of titanium silicide alloy films<sup>1,5-23</sup>. Here we shall refer to those which deal with a Si-Ti alloy film with a composition close to  $TiSi_2$ . The films are generally amorphous as deposited, and high temperatures (up to 800 C) are necessary to make a stable low resistivity titanium disilicide polycrystalline film. However Ti, either alone or as a silicide, reacts with most of the elements. The transformation kinetics of the silicon-titanium compounds are expected to be influenced by the presence of impurities, such as

oxygen, carbon and nitrogen. These impurities can be (i) incorporated in the metal film during deposition, (ii) incorporated in the polysilicon film used as a substrate in the polycide gate structure, or (iii) located at the metal/silicon interface.

However, transformation kinetics can also be affected by these impurities when they are present in the annealing ambient. The contributions of (i) to (iii) can be avoided with the current deposition systems, whereas the influence of the annealing ambient is more difficult to control and was found to be, for instance, the source of unwanted metal oxidation in tungsten hybridized films [24]. Metal oxides are also difficult to remove during patterning processes and degrade the electrical properties of the silicon oxide layers.

The purpose of the present work is to elucidate the microscopic mechanisms which are responsible for the crystallisation and formation of oxide of titanium silicide alloys when the annealing ambient is oxygen contaminated. A further aim is to find a method which gives a reliable and consistent process to avoid the problem of metal oxidation.

## SAMPLE PREPARATION AND EXPERIMENTAL TECHNIQUES

(100) boron doped (16-24 ohm-cm) 4 inch silicon wafers were used. The wafers were oxidized in wet oxygen to form about 1000 Å of SiO<sub>2</sub>. Subsequently 1800 Å of undoped polycrystalline silicon was deposited by low pressure chemical vapour deposition at about 625 C. The deposition was followed by a POCl<sub>3</sub> furnace doping at 920 C.

Alloy deposition was carried out in a Perkin Elmer 4400 rf-sputtering system. The base pressure was  $4 \times 10^{-5}$  Pa, and deposition was made at one Pa in Ar atmosphere. The sputtering system was equipped with a Meissner trap cooled to the temperature of liquid nitrogen. The required alloys were made by using separate titanium and silicon targets. The desired alloy composition was obtained by powering the two targets via power splitting so as to control the desired yield. The total thickness was 2500 Å with a typical deposition rate of 150 Å/min. Silicon wafers were mounted on a pallet rotating under the Ti and Si targets at 10 rpm. The combination of deposition and rotation rate produced individual layers a few angstrom thick which ensure a homogeneous film. No substrate heating was used during deposition, and it is estimated that the wafer temperature was lower than 100 C. A number of alloys with various compositions ranging from TiSi<sub>1.45</sub> to TiSi<sub>2.1</sub> have been prepared. The typical sample so produced was crystalline Si/SiO<sub>2</sub>/polySi/TiSi<sub>x</sub> deposited film. Furthermore a sputtered silicon cap 200 Å thick was deposited on two selected samples, the former silicon- and the latter titanium- rich. Samples were, therefore, crystalline Si/SiO<sub>2</sub>/polySi/TiSi<sub>x</sub>/Si cap deposited film.

Four different experimental techniques have here been used. (i) In-situ resistivity vs. temperature, (ii) Rutherford Backscattering Spectroscopy (RBS), (iii) Auger Electron Spectrometry (AES) and (iv) X-ray diffraction (XRD).

(i) Resistivity vs. temperature measurements were performed using a specially designed four point probe with tungsten tips, which is suitable for investigating metallurgical transformations<sup>25,26</sup>. In our case we were interested in the transfor-

mation from amorphous to bc C49 TiSi<sub>2</sub> and from C49 TiSi<sub>2</sub> to fc C54 TiSi<sub>2</sub>. A current of 1-10 mA was applied, and the power dissipated in the specimens less than 10<sup>-4</sup> W. Sample temperature was measured with a thermocouple placed in contact underneath the sample. (ii) 2 MeV <sup>4</sup>He<sup>+</sup> RBS in random conditions was used to obtain data on the atomic concentration and the depth distribution of the elements. (iii) AES was performed with a Varian scanning Auger electron spectrometer at 5 keV primary energy. Argon sputtering was performed with a differentially pumped ion gun operating at 2 keV. The whole spectrum in the energy region from 50 to 600 eV and from 1550 to 1700 eV was acquired in the derivative mode at 1 minute sputtering steps (about 50 Å in depth). In this way the p-p amplitude could be measured, and in addition the peak shape analyzed in order to obtain information on the different chemical bonds as well as to check for the presence of distribution of impurities. (iv) XRD was used to identify the formed compounds.

Annealing was performed either in argon ambient (purified by passing through a 800 C Ti bath) or in a mixture of nitrogen and oxygen. Oxygen contamination was obtained by adding 20% oxygen to nitrogen, the latter used as the carrier gas. The presence of nitrogen did not affect the results; this was checked in a number of samples where nitrogen was replaced by argon as the carrier gas with identical results. Samples were placed face to face in order to minimize possible contaminations during heat treatment. This procedure gave almost no additional contaminations from the annealing ambient, a fact proved by heating a pure Ti film and measuring its residual resistivity<sup>27</sup>.

## EXPERIMENTAL RESULTS

Table I shows the samples analyzed and some of their properties measured after slow heating in purified argon ambient up to 420 and 800 C. At the latter tem-

TABLE I  
Composition, thickness and resistivity of the various alloys investigated

Film structure and composition			silicide thickness (Å)		Room temperature resistivity (μohm/cm)	
as-deposited	420 C	800 C	as-dep.	800 C	as-dep.	800 C
amorphous TiSi <sub>1.45</sub>	TiSi + TiSi <sub>2</sub> bc	TiSi <sub>2</sub> fc	2400	2800	190	15
amorphous TiSi <sub>1.55</sub>	TiSi + TiSi <sub>2</sub> bc	TiSi <sub>2</sub> fc	2300	2600	220	15
amorphous TiSi <sub>1.6</sub>	TiSi + TiSi <sub>2</sub> bc	TiSi <sub>2</sub> fc	3100	3900	220	17
amorphous TiSi <sub>2.1</sub>	TiSi <sub>2</sub> bc	TiSi <sub>2</sub> fc	2200	2350	550	16.5

bc = orthorombic base centered

fc = orthorombic face centered

perature only the equilibrium  $\text{fc C54 TiSi}_2$  phase is produced, which exhibits a room temperature resistivity of about 15 microhm-cm.

The results for both capped or uncapped samples, and for annealing in purified argon or alternatively in oxygen-contaminated ambient, will be reported in four sections according to the four analytical techniques used, i.e. resistivity vs. temperature, RBS, AES and XRD.

(1) *In-situ resistivity vs. temperature measurements*

[a] *Annealing in purified argon*

The in-situ sheet resistance vs. temperature measured during heating at a constant rate of 1.5 C/min for two samples, namely  $\text{TiSi}_{2.1}$  and  $\text{TiSi}_{1.6}$ , the former Si- the latter Ti-rich, are reported in Fig. 1. Data were normalized to the room temperature value  $R_0$ . The arrows on the curves indicate the direction of temperature increase or decrease. At three different points, around 420, 700 and 800 C, heating was stopped and the sample was allowed to cool. The cooling curve is not superimposed

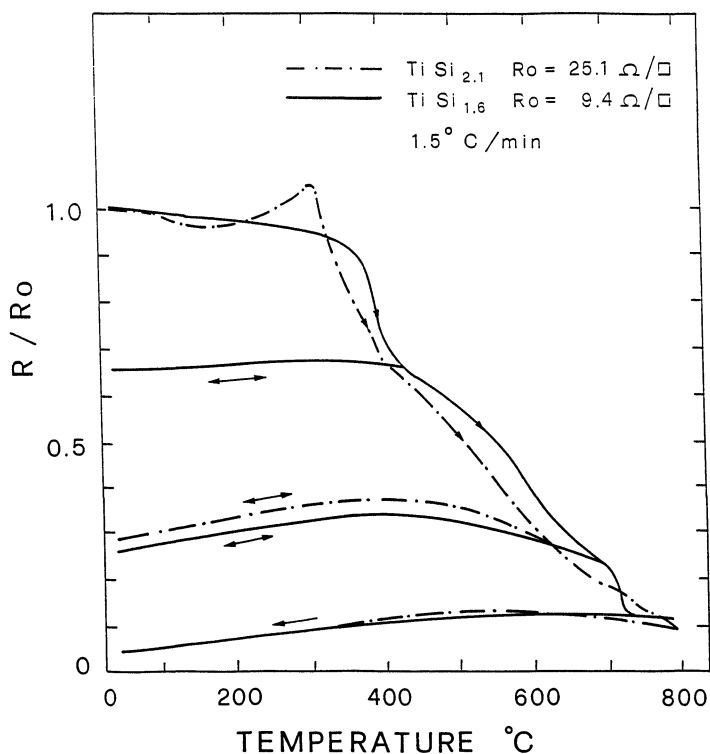


FIGURE 1 Temperature dependence of the normalized sheet resistance of  $\text{TiSi}_{2.1}$  and  $\text{TiSi}_{1.6}$  alloys measured in-situ during annealing at a constant rate of 1.5 C/min in a purified argon atmosphere.

on the one obtained during heating indicating that an irreversible metallurgical transformation has taken place.

However, once a certain temperature is reached, for instance 420 C, the cooling and the subsequent reheating curves do superimpose. This proves that no further metallurgical changes occur. We have investigated several samples: they all exhibit this same above behaviour, consequently we shall here only discuss in detail two alloys.

The overall behaviour for Si- and Ti-rich alloys are similar. The resistivity vs. temperature of the  $\text{TiSi}_{1.6}$  alloy presents fairly sharp drops. The first drop identifies the crystallisation temperature at about 400 C where the transition from amorphous to crystalline bc C49  $\text{TiSi}_2$  phase occurs (low temperature transition). The second drop occurs at about 730 C and identifies the transition from bc C49  $\text{TiSi}_2$  to fc C54  $\text{TiSi}_2$  phase (high temperature transition). The curve for the  $\text{TiSi}_{2.1}$  alloy presents an increase in resistance at around 300 C essentially due to the start of crystallisation. Resistivity exhibits an almost continuous decrease for temperatures above 300 C. However, even if the curve is almost featureless in this range, the slightly sharper behaviour at 350 C approximately identify this temperature as the crystallisation one. The above structural transformations are confirmed by our XRD data.

We have also made a kinetic study of the amorphous-crystalline transition at different heating rates, ranging from 0.5 to 10 C/min. On samples having the  $\text{TiSi}_{1.6}$  composition the results indicate a thermally activated process with an activation energy for crystallisation of about 1.3 eV. On samples having the  $\text{TiSi}_{2.1}$  composition the activation energy ranges from 0.8 to 1.5 eV. The latter uncertainty is due to a not sufficiently defined slope in the resistance vs. temperature plot exhibited by the Si-rich samples. The high temperature transition from bc C49  $\text{TiSi}_2$  to the fc C54  $\text{TiSi}_2$  phase is less well defined, from which only a rough estimate of an activation energy around 3 eV can be obtained, and that only for the Ti-rich samples.

[b] *Annealing in oxygen-bearing atmosphere, uncapped samples.*

Fig. 2 reports the in-situ sheet resistance vs. temperature measured during heating at a constant rate of 5 C/min for two samples, namely  $\text{TiSi}_{2.1}$  and  $\text{TiSi}_{1.45}$ , the former Si- the latter Ti-rich. The Si-rich samples exhibit an initial increase at 300 C, followed by a continuous fall, showing a crystallisation temperature of about 350 C, in agreement with the value obtained for annealing in purified argon. The same agreement is found for the Ti-rich samples, which exhibit a crystallisation temperature of 430 C. The nucleation temperature of the bc C49  $\text{TiSi}_2$  phase depends upon the film stoichiometry and is not affected by the annealing ambient. At higher temperatures the resistance behaviour is different from that observed in purified argon. This suggests that some other phenomena, different from the bc C49  $\text{TiSi}_2$  grain growth and bc C49  $\text{TiSi}_2$ -fc C54  $\text{TiSi}_2$  phase transition, takes place. At even higher temperatures (shaded area of Fig. 2) the measurements are not reproducible, mainly due to the loss of contacts caused by film oxidation, which is, at this level, evident from the sample colour even to the naked eye.

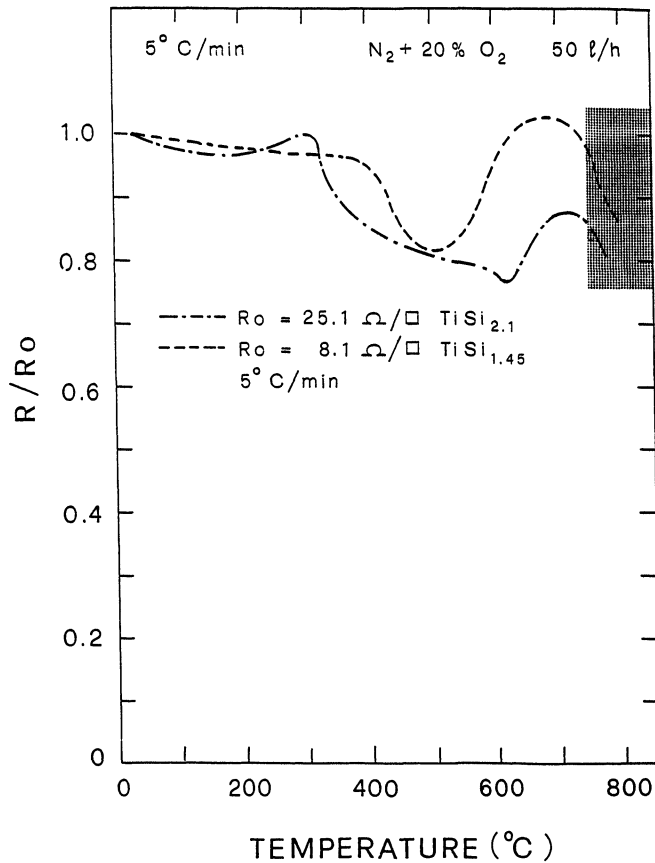


FIGURE 2 Temperature dependence of the normalized sheet resistance of  $\text{TiSi}_{2.1}$  and  $\text{TiSi}_{1.45}$  alloys measured in-situ during annealing at a constant rate of 5 C/min in an oxygen contaminated ambient.

[c] *Annealing in oxygen-bearing atmosphere, capped samples.*

Fig. 3 reports the in-situ sheet resistance vs. temperature measured during heating at a constant rate of 5 C/min and 10 C/min for a  $\text{TiSi}_{1.6}$  sample, covered by a 200 Å thick Si sputtered layer. The first drop at around 400 C evidences that the amorphous-crystalline transition occurs at this temperature. The second drop at 700 C indicates that the transition from the bc C49  $\text{TiSi}_2$  to the fc C54  $\text{TiSi}_2$  phase occurs quite abruptly. Both results are in agreement with those obtained on samples treated in argon atmosphere as reported in [a]. The same behaviour and agreement is obtained for Si-rich samples not shown here.

(2) *2 MeV  $^4\text{He}^+$  Rutherford Backscattering Spectrometry*

The nominal stoichiometry is confirmed by RBS measurements on samples as deposited, and RBS results ensure the in-depth sample uniformity. In addition,

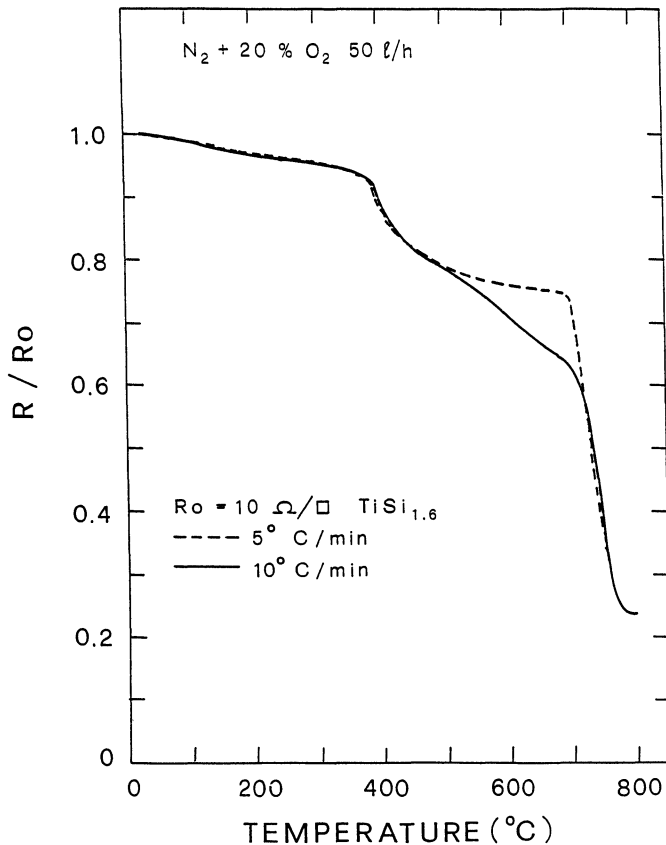


FIGURE 3 Temperature dependence of the normalized sheet resistance of a TiSi<sub>1.6</sub> Si-capped sample measured in-situ during annealing at a constant rate of 5 C/min and 10 C/min in an oxygen contaminated ambient.

RBS studies indicate a 1:2 Ti to Si ratio for Ti-rich samples, after annealing at 800 C in purified argon. A decrease in the polysilicon thickness and an increase in silicide layer thickness is also observed. No oxygen contribution to the RBS signal can be detected, where the sensitivity limit is about 5 at. %.

Two typical RBS spectra, the former for Si- and the latter for Ti-rich alloys are reported in Fig. 4a and 4b, respectively. Fig. 4a refers to 2210 Å thick TiSi<sub>2.1</sub> alloy, whereas Fig. 4b refers to a 2370 Å thick TiSi<sub>1.45</sub> alloy. In both figures the as-deposited state is compared with the one obtained after heating in oxygen contaminated atmosphere up to 800 C. The arrows indicate the position of the elements at the surface. Si in the inset should be read as polysilicon. The samples as prepared have the following structure: crystalline Si/SiO<sub>2</sub>/polySi/TiSi<sub>x</sub> deposited film. Since annealing only produces a modification in the two outermost layers, the inset in the figures shows these last two layers. The dip around channel 200 is due to the presence of the SiO<sub>2</sub> layer. Notice that after annealing the RBS spectra show (i)

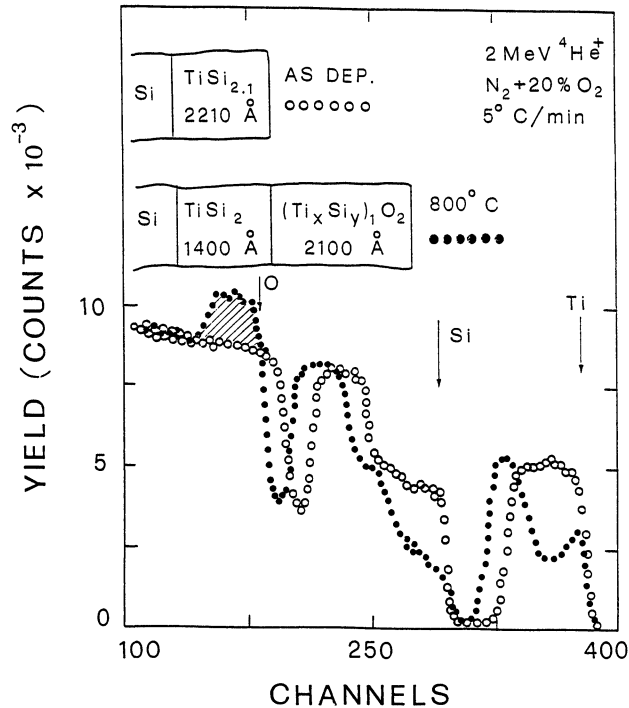


FIGURE 4a RBS spectra of the Si-rich sample as deposited and after annealing up to 800 C at a constant rate of 5 C/min in an oxygen contaminated ambient.

strong modification of Ti and Si peaks, and (ii) appearance of a squared uniform oxygen peak below channel 200 as evidenced by the shaded region. These facts indicate the presence of an oxidized layer on the sample, 2100 Å thick and 2370 Å thick for Si- and Ti-rich samples, respectively. We have obtained other RBS data from samples annealed in a purified Ar atmosphere, not here presented, all of which do not show presence of oxygen. Moreover these spectra show that, after annealing at 800 C, the polysilicon is consumed only in the Ti-rich samples, whereas upon annealing at 420 C such consumption is not exhibited.

Fig. 5 illustrates the RBS spectra obtained on silicon capped samples having a titanium rich alloy composition, as deposited and after annealing at 800 C in oxygen contaminated atmosphere. We note that oxygen is not detectable.

The sensitivity to oxygen in the present experimental arrangement is not optimized because the signal coming from oxygen at the surface is superimposed on the trailing edge of the signal coming from crystalline Si. The height of the Ti and Si peaks in the annealed samples indicate a TiSi<sub>2</sub> composition. Detection of Si atoms in the cap is limited both by the resolving power of our RBS technique and by the presence of oxygen contamination. This is confirmed by our AES data, later shown in Fig. 8a. The shapes of the Ti and Si peaks indicate a compound uniform in depth. Notice that, after annealing, the polysilicon peak has become narrower

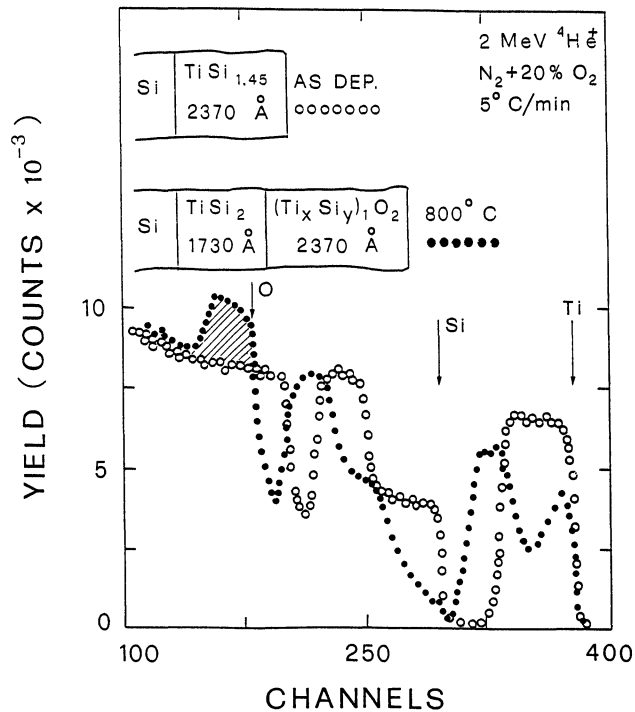


FIGURE 4b RBS spectra of the Ti-rich sample as deposited and after annealing up to 800 C at a constant rate of 5 C/min in an oxygen contaminated ambient.

and the Si signal in the silicide region increased. This shows that during the annealing process the polysilicon layer beneath the deposited TiSi<sub>1.6</sub> layer has been partially consumed in the production of silicide. This is furthermore confirmed by the reduced and widened Ti signal.

### (3) Auger electron spectroscopy

Fig. 6 shows the depth profile obtained by AES and Ar sputtering of the TiSi<sub>2.1</sub> sample heated in the oxygen contaminated atmosphere up to 800 C. The atomic concentration scale is only valid in the oxygen-free titanium silicide layer, because the relative elemental sensitivity factors obtained in a standard TiSi<sub>2</sub> layer (calibrated with RBS) were used. The data confirm the results of Fig. 4: in fact the outermost layer is consist of a combination of Si, Ti and O, whereas the innermost layer is essentially TiSi<sub>2</sub> with only a very light oxygen contamination. All other samples which have been analyzed by use with AES gave elemental depth distributions in agreement with our RBS spectra.

To obtain information on the chemical bonding of the various elements, the whole AES spectra have been recorded during the depth profile measurements in the points marked a, b and c in Fig. 6, and they are reported in Fig. 7.

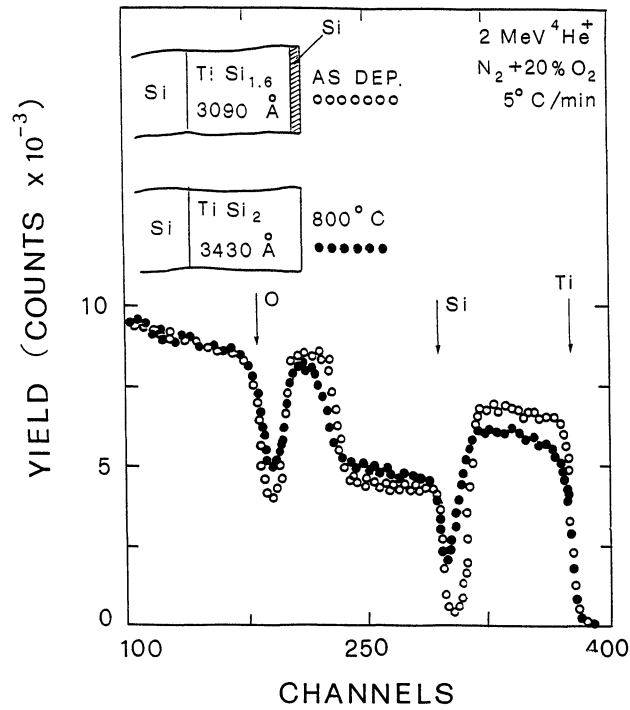


FIGURE 5 RBS spectra of the Si-capped sample as deposited and after annealing up to 800 C at a constant rate of 5 C/min in an oxygen contaminated ambient.

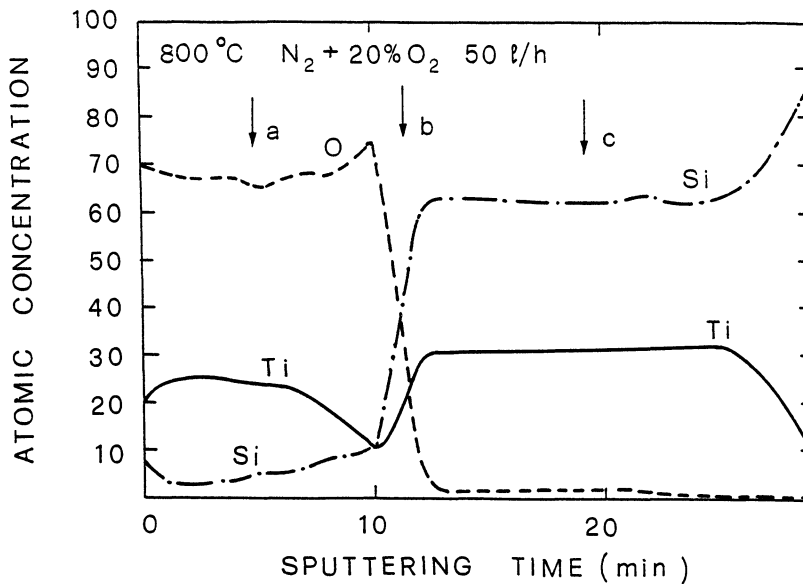


FIGURE 6 AES profile of the TiSi<sub>2.1</sub> sample taken after annealing up to 800 C at a constant rate of 5 C/min in an oxygen contaminated ambient. The arrows labelled a, b and c show the point where a whole Auger spectrum was recorded.

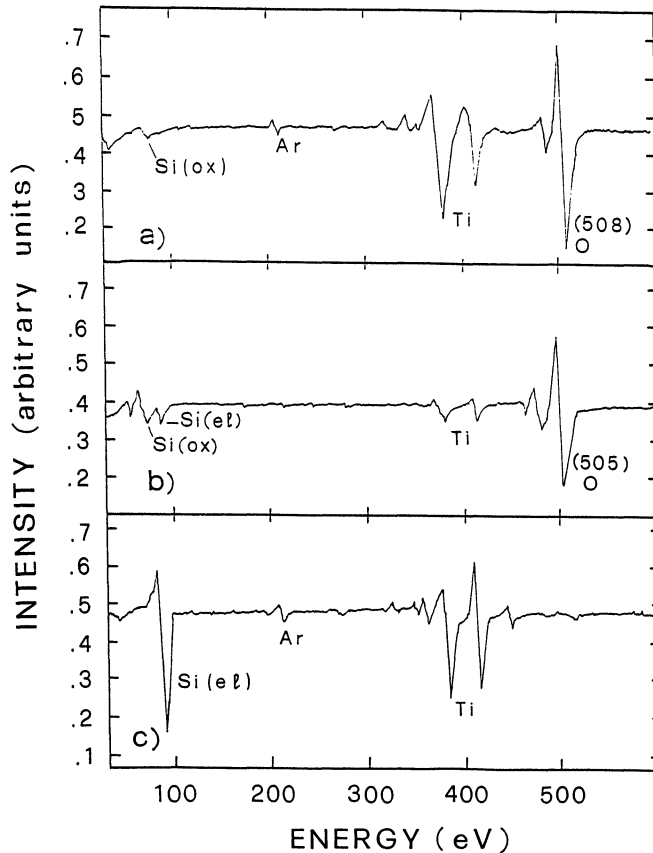


FIGURE 7 AES spectra recorded during the depth profile of the sample of Fig. 6. a), b) and c) refer to the various sample regions pointed to by the arrows in Fig 6.

Fig. 7c shows the spectrum related to the film sampled at full depth. The Si and Ti lineshapes are identical to those reported in the literature for metallic  $\text{TiSi}_2$ <sup>28,29</sup>. Moreover the ratio between the two Ti peak intensities at 418 eV and 380 eV is about unity, as expected<sup>30</sup>.

Fig. 7a shows the spectrum related to the film sampled at the outermost layer. A mixture of silicon oxide (presumably  $\text{SiO}_2$ ) with titanium oxide  $\text{TiO}_x$  (where  $x$  is close to two) is here shown. The presence of  $\text{SiO}_2$  is mostly inferred by the position of the Si peak placed at 76 eV which is confirmed by the peak at 91 eV, as shown in Fig. 7c, which is unambiguously due to pure Si. The oxygen peak from  $\text{SiO}_2$ , located at 505 eV, is hidden in the one located at 508 eV; the latter being attributed to the titanium-oxygen bond. The ratio between the two LMM titanium peaks at 418 and 380 eV is less than one, which is typical of titanium oxide<sup>31</sup> from which the presence of  $\text{TiO}_x$  can be inferred.

Fig. 7b shows the spectrum related to the film sampled at a depth intermediate between the surface a) and the full depth c). This layer consists of a mixture of  $\text{TiSi}_2$  and silicon oxide. The presence of  $\text{TiSi}_2$  is deduced by the lineshapes of Ti

which have a peak intensity ratio close to one and by the silicon peak which is located at 91 eV. Both these features agree with the findings shown in Fig. 7c. Silicon oxide is revealed by the position of the silicon peak at 76 eV<sup>32</sup> and by the displacement of the oxygen peak from 508 eV to 505 eV. Note that TiO<sub>x</sub> is not detectable at the interface, even if its presence in very small quantities could be hidden by the 505 eV oxygen peak.

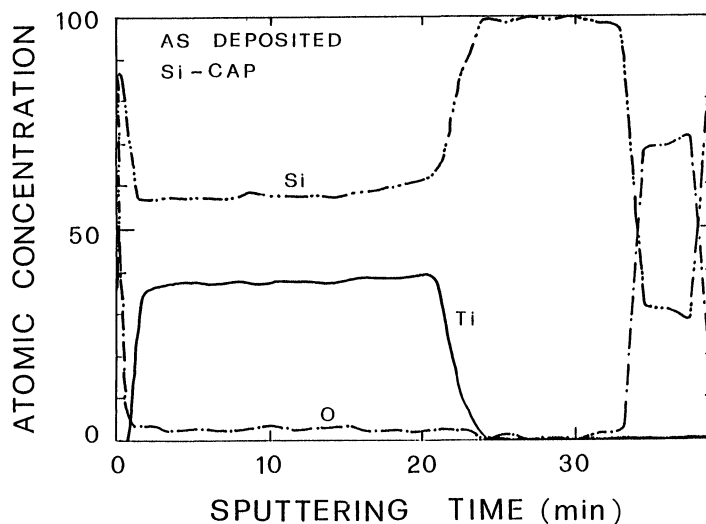


FIGURE 8a AES profile of the Si-capped sample taken as deposited before annealing.

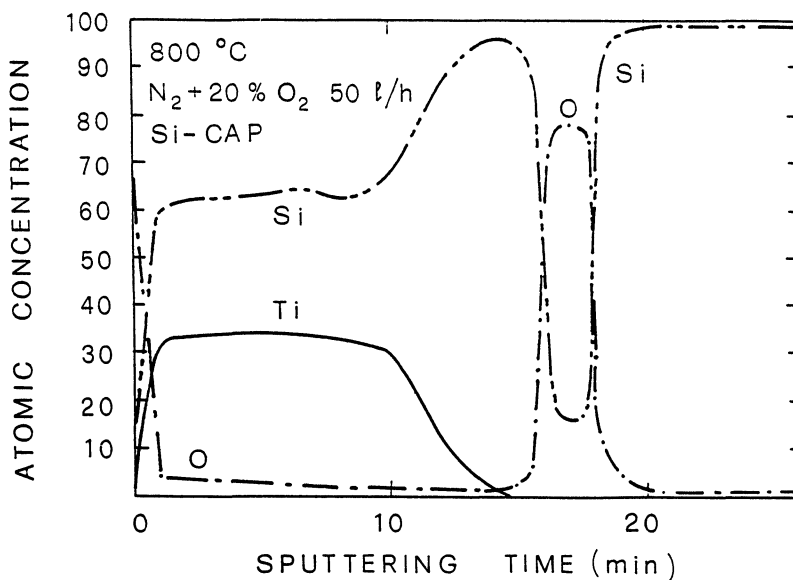


FIGURE 8b AES profile of the Si-capped sample of Fig 8a taken after annealing up to 800 C at a constant rate of 5 C/min in an oxygen contaminated ambient.

The effect of a thin layer of silicon sputtered on top of the silicide layer for a  $\text{TiSi}_{1.6}$  sample (Si-cap) is shown in Fig. 8.

Fig. 8a shows the depth profiles related to the film as-deposited. The effect of the presence of the silicon cap is here clearly shown: some oxygen is detected only at the surface in the thin native silicon dioxide layer. Fig. 8b shows the depth profiles related to the film which had undergone heating in oxygen contaminated atmosphere up to 800 C. It can be here seen that, after heating, only a very thin native silicon oxide layer is grown at the sample surface, in contrast with the thick mixed oxide found in the non-capped samples as shown in Fig. 6. Moreover, the film composition reaches the stoichiometric 1:2 ratio, due to the reaction of excess Ti with Si from the underlying polysilicon.

Fig. 9 shows AES spectra obtained for a Si-capped sample which had undergone the thermal treatment in oxygen-bearing atmosphere at 875 C for 120 min. The growth of a thick silicon dioxide layer is exhibited with the remarkable result that the Ti content in the film is negligibly small.

#### (4) x-ray diffraction

XRD data are reported in Figs. 10a and 10b, the former for Si-rich samples, the latter for the Ti-rich ones, both as deposited and after heating in purified Ar atmosphere up to 420 and 800 C. Both types of samples as deposited are amorphous and the only peaks come from the polysilicon substrate. Upon heating up to 420 C it is seen that only the bc C49  $\text{TiSi}_2$  phase is present for the silicon-rich samples (Fig. 10a), while both the bc C49  $\text{TiSi}_2$  and the  $\text{TiSi}$  phases are detected at that

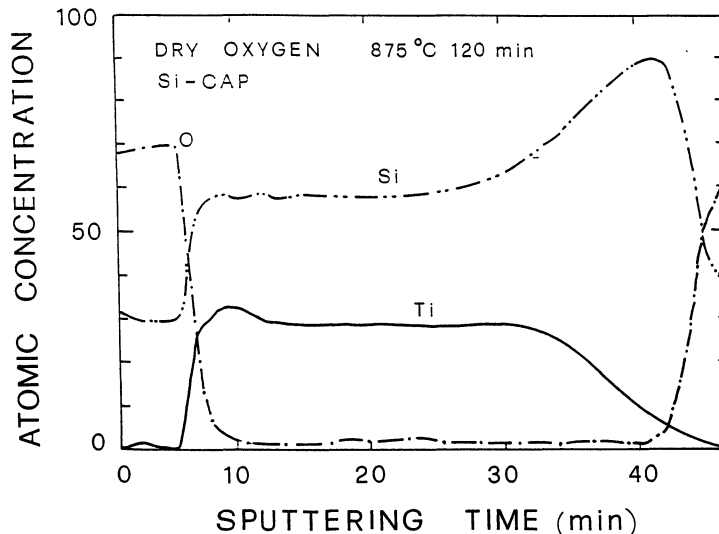


FIGURE 9 AES profiles of the Si-capped sample taken after a thermal treatment in an oxygen-bearing atmosphere at 875 C for 120 min.

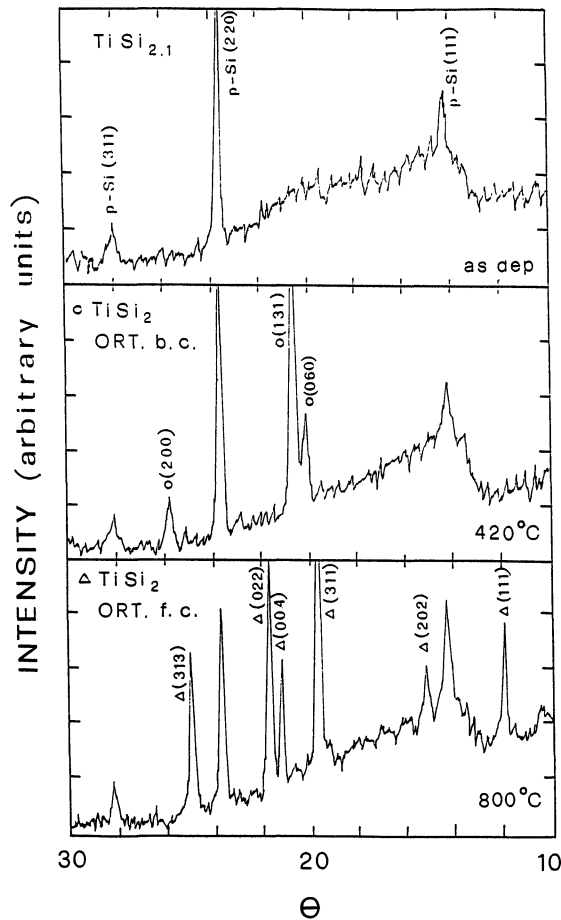


FIGURE 10a XRD spectra taken in a Si-rich sample as deposited (upper figure), after heating in purified atmosphere up to 420 C (middle figure) and up to 800 C (lower figure).

temperature in the titanium-rich samples (Fig. 10 b). XRD spectra also show that, upon annealing at 800 C, for both types of samples only the fc C54  $\text{TiSi}_2$  phase is produced.

Capped and uncapped samples have also been XRD analyzed after annealing in oxygen-bearing atmosphere up to 800 C. Both type of samples exhibit the presence of the fc C54  $\text{TiSi}_2$  phase. The uncapped samples show peaks with lower intensities than for the capped ones reflecting the consumption of the silicide film caused by oxidation.

## DISCUSSION AND CONCLUSIONS

We have seen that the amorphous films of titanium-silicon alloys as deposited exhibit a high electrical resistivity, and that suitable heat treatments are necessary to

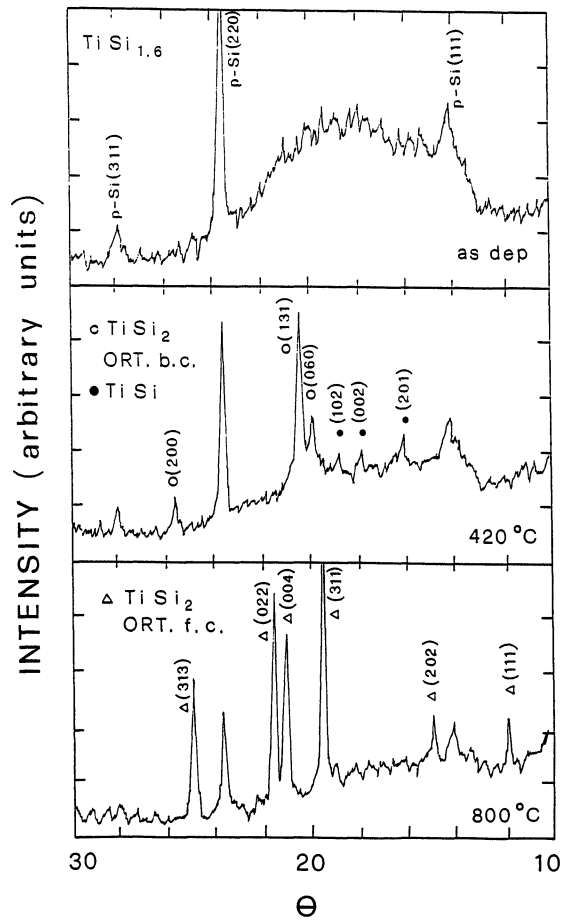


FIGURE 10b XRD spectra taken in a Ti-rich sample as deposited (upper figure), after heating in purified atmosphere up to 420 C (middle figure) and up to 800 C (lower figure).

achieve the desired low values. The sheet resistivity vs. temperature dependence shown in Figs. 2-3 can be considered as a reference for the behaviour of the  $\text{TiSi}_x$  alloy system undergoing an annealing process, for  $x$  in the neighbourhood of two. Both alloys, Si- and Ti-rich exhibit two sharp drops in the resistivity vs. temperature plots. The first evidences the low temperature transition which occurs around 350-400 C. According to XRD analysis, it corresponds to the transformation from the amorphous to crystalline bc C49  $\text{TiSi}_2$  phase. The second illustrates the high temperature transition which occurs around 700-800 C and corresponds to the phase transformation from bc C49  $\text{TiSi}_2$  to fc C54  $\text{TiSi}_2$ . This latter phase is the desired equilibrium phase and has the lowest value of sheet resistivity of about 15-17 microhm-cm as shown in Table I. This value is in agreement with those reported in the literature which range from 10 to 20 microhm-cm<sup>33</sup>.

Table I shows that a heat treatment up to 800 C of a film made of evaporated

Si and Ti on a polysilicon substrate (crystalline Si/SiO<sub>2</sub>/poly Si/TiSi<sub>x</sub> with x ranging from 1.45 to 2.1) always produces TiSi<sub>2</sub>. At low temperatures, around 420 C, a Si-rich film produces stoichiometric TiSi<sub>2</sub> plus presumably silicon segregations, whereas a Ti-rich film produces both TiSi<sub>2</sub> and TiSi. These results are in agreement with what is generally expected when a thermal treatment is made on non-stoichiometric alloys deposited on an inert substrate. However our substrate is not inert but a polysilicon: the production of both TiSi<sub>2</sub> and TiSi in Ti-rich alloys arise at low temperatures because the polysilicon substrate cannot supply adequate amount of silicon to the alloy to feed the reaction necessary to produce TiSi<sub>2</sub>. This deduction is supported by the literature<sup>8</sup> where at least 500 C is needed to achieve a Si-transport activated reaction in the formation of TiSi<sub>2</sub> by thin Ti films on Si.

Measurements at various heating rates have revealed the activation energy for crystallisation and for phase transformation from bc C49 TiSi<sub>2</sub> to fc C54 TiSi<sub>2</sub>. The activation energy for crystallisation was found to be 1.3 eV in Ti-rich alloys and about 0.8-1.5 eV in Si-rich ones, both in agreement with reported data<sup>34,35</sup> and attributed to the growth of silicide grains. That for phase transformation was found to be 3 eV, which is in between the values reported by the literature: 1.8 eV<sup>23</sup> and 4.4 eV<sup>20,35</sup>. The lack of precision in the above figures is not surprising since it derives from the inherently insufficient sharpness in the change of resistivity vs. temperature plots.

Ti is very reactive with oxygen and forms various kinds of oxides<sup>36</sup>. Heavy oxidation effects are clearly evident at 500 C in Fig. 2, but presumably this starts at even lower temperatures. Several experimental findings suggest that a Si-rich environment inhibits metal oxidation. (i) In the case of TiSi<sub>2</sub> it is necessary to have at the surface a segregation of silicon in order to avoid the formation of titanium oxide<sup>37-39</sup> (ii) Our AES spectra of Fig. 7b taken in the regions in which the material is Si-rich show that oxygen is mainly bound to silicon and forms silicon dioxide. (iii) It has been found that the Si-rich compounds form silicon oxide more easily than metal-rich compounds in near noble metal silicides<sup>40,41</sup>.

An excess of silicon could be attained via dynamic conditions by taking into account the rate of silicon transport through the silicide. This requires a source of material, polysilicon for instance, and sufficiently high temperatures for the transport. However this cannot be met in the specific case of TiSi<sub>2</sub>. In fact, according to the diffusion data<sup>8</sup>, the temperature for the transport of Si in silicides should be above 500-550 C which is higher than that at which TiSi<sub>2</sub> starts to oxidize.

Therefore, to avoid metal oxidation, titanium should not come into contact with oxygen in the low temperature range during the annealing process. A possible solution is obviously to operate the annealing in an oxygen-free ambient, which is however very difficult to meet in normal industrial environments. A more practical approach is to apply a silicon film cap on top of the sample before annealing. In fact we have seen that a 200 Å silicon film cap has the function of decoupling the alloy from incoming oxygen even during the low temperature range of the annealing process, as proven by our AES result shown in Figs. 7, 8 and 9 and by the sheet resistivity vs. temperature behaviour shown in Fig. 3. Once the required low resistivity TiSi<sub>2</sub> film is attained, the presence of such a cap also permits, if required, the sample to undergo an oxidation process intended to form a uniform silicon

oxide film through the complete oxidation of the silicon cap without appreciably contaminating the underlying TiSi<sub>2</sub> alloy.

In conclusion, by using mostly in-situ resistivity measurements on amorphous Ti-Si alloys with various compositions we have shown that:

(i) During annealing in a purified argon ambient the alloys crystallize around 450 C in the bc C49 TiSi<sub>2</sub> phase with an activation energy of 1.3 eV for Ti-rich and 0.8-1.5 eV for Si-rich alloys. At high temperatures, around 700 C, the bc C49 TiSi<sub>2</sub> phase transforms into the fc C54 TiSi<sub>2</sub> (the desired low resistivity equilibrium phase) with an activation energy of 3 eV.

(ii) Annealing in oxygen contaminated atmosphere produces the formation of oxides having an atomic composition Si<sub>1-x</sub> Ti<sub>x</sub> O<sub>2</sub> which seem to be a mixture of SiO<sub>2</sub> and TiO<sub>x</sub>. Oxidation occurs mostly at low temperatures, around 500 C.

(iii) In oxygen contaminated ambients, the presence of a 200 Å thin silicon capping layer deposited on the silicide alloy, allows the formation of the required low resistivity TiSi<sub>2</sub> without appreciable formation of titanium oxides.

(iv) Such a cap also allows a uniform silicon oxide film not appreciably contaminated with the metal to form.

#### REFERENCES

1. S.P. Murarka, "Silicides for VLSI Applications" (Academic Press, New York, 1983).
2. M.-A. Nicolet and S.S. Lau, chapter in "VLSI Electronics: Microstructure Science", N. Einspruch, Series Editor, Supplement A - "Material and Process Characterisation", Graydon Larrabee, guest Editor (Academic Press, New York, 1985).
3. T.C. Chou, C.Y. Wong, and K.N. Tu, "Lattice imaging of metastable TiSi<sub>2</sub>.", *J. Appl. Phys.* 62, 2275 (1987).
4. H.J.W. van Houtum and I.J.M.M. Raaijmakers, "First phase nucleation and growth of titanium disilicide with an emphasis on the influence of oxygen.", *Mat. Res. Soc. Symp. Proc.* 54, 37 (1986).
5. "Thin Films - Interdiffusion and Reactions.", Edtrs. J.M. Poate, K.N. Tu and J.W. Mayer (John Wiley and Sons, New York, 1978).
6. R.W. Bower and J.M. Mayer, "Growth kinetics observed in the formation of metal silicides on silicon." *Appl. Phys. Lett.*, 20, 359 (1972).
7. S.P. Murarka and D.B. Fraser, "Silicide formation in thin cosputtered (titanium + silicon) films on polycrystalline and SiO<sub>2</sub>." *J. Appl. Phys.* 51, 342 (1980).
8. L.S. Hung, J. Gyulai, J.W. Mayer, S.S. Lau and M. Nicolet, "Kinetics of TiSi<sub>2</sub> formation by thin Ti films on Si." *J. Appl. Phys.* 54, 5076 (1983).
9. E.D. Adams, K.Y. Ahn and S.B. Brodsky, "Formation of TiSi<sub>2</sub> and TiN during nitrogen annealing of magnetron sputtered Ti films." *J. Vac. Sci. and Technol.* A3, 2264 (1985).
10. G. Ottaviani and J.M. Mayer in "Reliability and Degradation - Semiconductor Devices and Circuits." Edtrs. M.J. Hoves and D.V. Morgan (John Wiley and Sons, New York, 1981), p. 105.
11. H. Kato and Y. Nakamura, "Solid state reactions in titanium thin films of silicon." *Thin Solid Films* 34, 135 (1976).
12. A. Guldan, V. Schiller, A. Steffen and P. Balk, "Formation and properties of TiSi<sub>2</sub> films." *Thin Solid Films* 100, 1 (1983).
13. M. Berti, A.V. Drigo, C. Cohen, J. Siejka, G.C. Bentini, R. Nipoti and S. Guerri, "Titanium silicide formation: effect of oxygen distribution in the metal film." *J. Appl. Phys.* 55, 3558 (1984).
14. H.-L. Hoo and J.B. Avins, "Compound sputtering cathodes of refractory metal silicides and thin film produced." *J. Vac. Sci. Technol.* B3, 1692 (1985).
15. C.G. Sridhar, R. Chow and G. Nocerino, "Sputter depositon of refractory metal silicides from cold-pressed vacuum-sintered targets." *Thin Solid Films* 140, 51 (1986).

16. M.L. Hitchman, A.D. Jobson and L-F.T. Kwakman, "Some considerations of the thermodynamics and kinetics of the chemical vapour deposition of tungsten." *Appl. Surf. Science* 38, 312 (1989).
17. J.L. Regolini, D. Bensahel, G. Bomchil and J. Mercier, "Selective layers of TiSi<sub>2</sub> deposited without substrate consumption in a cold wall LPCVD reactor." *Appl. Surf. Science* 38, 408 (1989).
18. M.J. Kemper and P.H. Oosting, "Crystallization and resistivity of amorphous titanium silicide films deposited by coevaporation." *J. Appl. Phys.* 53, 6214 (1982).
19. A. Steffen, J. Korec, M. Maier and P. Balk, "Loss of material from TiSi<sub>2</sub> films during annealing in hydrogen." *Thin Solid Films* 130, 297 (1985).
20. R.D. Thomson, H. Takai, P. Psaras and K.N. Tu, "Effect of a substrate on the phase transformation of amorphous TiSi<sub>2</sub> thin films." *J. Appl. Phys.* 61, 540 (1987).
21. R. Beyers, R. Sinclair and M.E. Thomas, "Tem studies of cosputtered TiSi<sub>2</sub> films containing excess silicon." *Mater. res. Soc. Symp. Proc.* 14, 423 (1983).
22. H.O. Blom, S. Berg, M. Ostling, C.S. Petersson, V. Deline and F.M. d'Heurle, "Titanium silicide films prepared by reactive sputtering." *J. Vac. Sci. Technol.* B3, 997 (1985).
23. S.P. Murarka and D.B. Fraser, "Silicide formation in thin cosputtered (titanium + silicon) films on polycrystalline silicon and SiO<sub>2</sub>." *J. Appl. Phys.* 51, 350 (1980).
24. L. Bacci, G. DeSanti and G. Queirolo, "Boundary conditions to oxidation of WSi<sub>2</sub>/polysilicon structures" in "Tungsten and other refractory metals for VLSI Application, IX", Edited by R.S. Blewer (MRS, Pittsburgh, Pa., 1989) p. 353.
25. L.P. Van der Pauw, "A method of measuring specific resistivity and Hall effect of discs of arbitrary shape." *Philips Res. Rep.* 13, 1 (1981).
26. T. Tien, G. Ottaviani and K.N. Tu, "Temperature dependence of structural and electrical properties of Ta-Si thin alloy films." *J. Appl. Phys.* 54, 7047 (1983).
27. G. Ottaviani, F. Nava, G. Queirolo, G. Iannuzi, G. DeSanti and K.N. Tu, "Low temperature oxygen dissolution in titanium." *Thin Solid Films* 146, 201 (1987).
28. J.A. Roth and C.R. Crowell, "Application of Auger electron spectroscopy to studies of the silicon/silicide interface." *J. Vac. Sci. Technol.* 15, 1317 (1978).
29. V. Atzordt, W. Titel, Th. Wirth and H. Lange, "AES study of thin films MoSi<sub>2</sub>." *Phys. Stat. Sol.* (a)75, k15 (1983).
30. E.K. Broadbent, A.E. Morgan, B. Coulman, I.-W. Huang and A.E.T Kuiper, "Characterization of titanium silicide films formed by composite sputtering and rapid thermal annealing." *Thin Solid Films*, 151, 51 (1987).
31. M. Clement, J.M. Sanz and J.M. Martinez-Duart, "An AES study of the oxidatin of TaSi<sub>x</sub> after bombardment with Ar<sup>+</sup> ions of different energies." *Surf. Interf. Anal.* 14, 473 (1989).
32. B. Carriere and J.P. Deville, "The early stages of oxygen adsorption on silicon surfaces as seen by electron spectroscopy." *Surf. Sci.* 80, 278 (1979).
33. F.M. d'Heurle, P. Gas, I. Engstroem, S. Nygren, M. Ostling and G. Petersson,, "The two crystalline structure of TiSi<sub>2</sub>: identification and resistivity." *IBM Research Report RC 11151 (#50067) Solid State Physics* 5/3/85 (1985).
34. I.J.M.M. Raaijmaker, A.H. Reader and H.J.W. van Houton, "Nucleation and growth of titanium silicide studied by in situ annealing in a transmission electron microscope." *J. Appl. Phys.* 61, 2527 (1987).
35. R.D. Thompson, H. Takai, P.A. Psaras and K.N. Tu, "Effect of a substrate on the phase transformations of amorphous TiSi<sub>2</sub> thin films." *J. Appl. Phys.* 61, 540 (1987).
36. W.G. Moffatt, "Binary Phase Diagrams Handbook" (General Electric Company, 1976), Supplements.
37. J.-R. Chen, Y.-C. Liu and S.-D. Chu, "Oxidation of titanium disilicide on polycrystalline silicon." *J. Electron Mat.* 11, 355 (1982).
38. F. d'Heurle, E.A. Irene and C.Y. Ting, "Oxidation of silicide thin films: TiSi<sub>2</sub>." *Appl. Phys. Lett.* 42, 361 (1983).
39. G. Valyi, L. Zhaokang, A. Steffen, M. Maier, P. Balk and J. Gyulai, "Oxidation behaviour of double layers of TiSi<sub>2</sub> on polycrystalline silicon." *Thin Solid Films*, 116, 383 (1984).
40. S. Valeri, "AES and XPS study of Cr-silicide surfaces behaviour under ion bombardment and oxygen exposure." *Le Vide, les couches Minces* 42, 13 (1987).
41. S. Valeri, V. del Pennino, P. Lomellini and P. Sassaroli, "Oxygen chemisorption and oxide formation on Ni silicides surfaces at room temperature." *Surf. Sci.* 145, 375 (1987).



**Hindawi**

Submit your manuscripts at  
<http://www.hindawi.com>

